SANDIA REPORT

SAND2018-7447
Unlimited Release
Printed July 2018

An Exchange-Correlation Functional Capturing Bulk, Surface, and Confinement Physics

Attila Cangi

Prepared by
Sandia National Laboratories
Albuquerque, New Mexico 87185 and Livermore, California 94550

Sandia National Laboratories is a multimission laboratory managed and operated by National Technology and Engineering Solutions of Sandia, LLC., a wholly owned subsidiary of Honeywell International, Inc., for the U.S. Department of Energy's National Nuclear Security Administration under contract DE-NA0003525.

Sandia National Laboratories

Issued by Sandia National Laboratories, operated for the United States Department of Energy by National Technology and Engineering Solutions of Sandia, LLC.

Available to DOE and DOE contractors from
U.S. Department of Energy
Office of Scientific and Technical Information
P.O. Box 62
Oak Ridge, TN 37831

Telephone: (865) 576-8401
Facsimile: (865) 576-5728
E-Mail: reports@osti.gov
Online ordering: http://www.osti.gov/scitech

Available to the public from
U.S. Department of Commerce
National Technical Information Service
5285 Port Royal Rd
Springfield, VA 22161

Telephone: (800) 553-6847
Facsimile: (703) 605-6900
E-Mail: orders@ntis.gov
Online ordering: http://classic.ntis.gov/help/order-methods/

SAND2018-7447
Printed July 2018
Unlimited Release

An Exchange-Correlation Functional Capturing Bulk, Surface, and Confinement Physics

Attila Cangi
Multiscale Science Department
Center for Computing Research
Sandia National Laboratories
P.O. Box 5800
Albuquerque, NM 87185-1321
acangi@sandia.gov

Abstract

Due to its balance of accuracy and computational cost, density functional theory has become the method of choice for computing the electronic structure and related properties of materials. However, present-day semilocal approximations to the exchange-correlation energy of density functional theory break down for materials containing d and f electrons.

In this report we summarize our progress in addressing this issue. We describe the construction of the BSC exchange-correlation functional within the subsystem functional formalism which enables us to capture bulk, surface, and confinement physics with a single exchange-correlation functional. We report on the initial assessment of this functional within the jellium surface system and demonstrate that the BSC functional captures the confinement physics more accurately than standard semilocal exchange-correlation functionals. We conclude by outlining our future research objectives which focus on refining the functional form of the BSC functional and achieving significantly more accurate energetics of materials containing f and d electrons than existing semilocal functionals.

Acknowledgments

We acknowledge valuable discussions with Ann Wills at the Los Alamos National Laboratory on techniques regarding functional construction.

Sandia National Laboratories is a multimission laboratory managed and operated by National Technology & Engineering Solutions of Sandia, LLC, a wholly owned subsidiary of Honeywell International Inc., for the U.S. Department of Energys National Nuclear Security Administration under contract DE-NA0003525. This paper describes objective technical results and analysis. Any subjective views or opinions that might be expressed in the paper do not necessarily represent the views of the U.S. Department of Energy or the United States Government.

Contents

Appendix

List of Figures

List of Tables

Nomenclature

BO Born-Oppenheimer

DFT Density functional theory

ELF Electron localization function

GGA Generalized gradient approximation

HK Hohenberg-Kohn

HOG Harmonic Oscillator Gas

KS Kohn-Sham

LDA Local density approximation

MGGA Meta-generalized gradient approximation

PES Potential energy surface

XC Exchange-correlation

Chapter 1

Introduction

Density Functional Theory (DFT) has become an indispensable tool for predicting materials properties and guiding novel material synthesis[13]. However, current implementations of DFT break down for the heavier elements, such as rare earths, lanthanides, actinides, and the transition metal oxides. These classes of materials are crucially important to DOE nuclear weapons/nuclear security mission. In particular, understanding the chemical properties of d- and f-electron systems is in alignment with DOE's interest in heavy element chemistry research.

Materials properties can be deduced from their electronic structure, which in turn can be calculated using DFT-based methods. The properties of materials composed entirely of lighter elements, such as aluminum, governed by s and p electrons, can be accurately predicted using existing DFT techniques. However, DFT calculations with semilocal exchange-correlation functionals (GGAs and MGGAs) for elements governed by d and f electrons are inaccurate. A patchwork of workarounds termed beyond-DFT methods such as hybrid functionals[7, 41], DFT+U[3, 2, 56], Dynamical Mean Field Theory[24], the Gutzwiller approximation[29], and the GW approximation[5] have been developed and applied in order to increase the accuracy. However, these workarounds are computationally expensive which limits their utility for computational materials science investigations.

In this report we summarize the current status of our effort in developing an exchange-correlation (XC) approximation in order to make DFT calculations predictive for all materials, including these important material classes. This work will allow the extension of model-based design and engineering to all materials, including those with heavier elements in their composition.

Chapter 2

Theoretical Background

2.1 The Electronic Structure Problem within the Born-Oppenheimer Approximation

Consider a unit cell of a material composed of N^{e} electrons with collective electronic coordinates $\{\mathbf{r}\} = \{\mathbf{r}_1, \ldots, \mathbf{r}_{N^{\mathrm{e}}}\}$ and N^{n} nuclei with masses M_I, charges Z_I, and collective nuclear coordinates $\{\mathbf{R}\} = \{\mathbf{R}_1, \ldots, \mathbf{R}_{N^{\mathrm{n}}}\}$. Its non-relativistic Hamiltonian[1] is given by

$$\hat{H} = \hat{H}^{\mathrm{BO}}(\{\mathbf{r}\}, \{\mathbf{R}\}) + \hat{T}^{\mathrm{n}}(\{\mathbf{R}\}), \tag{2.1}$$

where the Born-Oppenheimer Hamiltonian is defined as

$$\hat{H}^{\mathrm{BO}}(\{\mathbf{r}\}, \{\mathbf{R}\}) = \hat{T}^{\mathrm{e}}(\{\mathbf{r}\}) + \hat{W}^{\mathrm{ee}}(\{\mathbf{r}\}) + \hat{W}^{\mathrm{en}}(\{\mathbf{r}\}, \{\mathbf{R}\}) + \hat{W}^{\mathrm{nn}}(\{\mathbf{R}\}) \,. \tag{2.2}$$

The contributions to the Born-Oppenheimer Hamiltonian are

$$\hat{T}^{\mathrm{e}} = -\sum_{j=1}^{N^{\mathrm{e}}} \frac{\nabla_j^2}{2}, \quad \hat{T}^{\mathrm{n}} = -\sum_{J=1}^{N^{\mathrm{n}}} \frac{\nabla_J^2}{2M_J}, \tag{2.3}$$

denoting the kinetic energy operator of the electrons and nuclei and

$$\hat{W}^{\mathrm{ee}} = \sum_{\substack{i,j=1 \\ i>j}}^{N^{\mathrm{e}}} \frac{1}{|\mathbf{r}_i - \mathbf{r}_j|}, \quad \hat{W}^{\mathrm{en}} = -\sum_{i}^{N^{\mathrm{e}}} \sum_{I}^{N^{\mathrm{n}}} \frac{Z_I}{|\mathbf{r}_i - \mathbf{R}_I|}, \quad \hat{W}^{\mathrm{nn}} = \sum_{\substack{I,J=1 \\ I \neq J}}^{N^{\mathrm{n}}} \frac{Z_I Z_J}{2|\mathbf{R}_I - \mathbf{R}_J|}, \tag{2.4}$$

denoting the electron-electron, the electron-nuclear, the nuclear-nuclear interactions.

The Schrödinger equation for the system of coupled electrons and nuclei

$$\hat{H}\,\Psi(\{\mathbf{r}\}, \{\mathbf{R}\}) = E\,\Psi(\{\mathbf{r}\}, \{\mathbf{R}\}) \tag{2.5}$$

determines the full electron-nuclear wave function Ψ.

[1] in atomic units here and thereafter, where $e^2 = \hbar = m^{\mathrm{e}} = 1$, so that lengths are expressed in Bohr radii and energies are in hartree.

The most basic approximation to the Schrödinger equation of coupled electrons and nuclei is the Born-Oppenheimer approximation [12, 11] which allows us to decouple the electronic and nuclear degrees of freedom and to write the total electron-nuclear wave function in factorized form as

$$\Psi(\{\mathbf{r}\},\{\mathbf{R}\}) \approx \chi_{J,j}(\{\mathbf{R}\})\,\Phi_j(\{\mathbf{r}\},\{\mathbf{R}\})\,. \tag{2.6}$$

This leads to two coupled equations, one for the electrons and the other for the nuclei. The electronic Schrödinger equation

$$\hat{H}^{\mathrm{BO}}\,\Phi_j(\{\mathbf{r}\},\{\mathbf{R}\}) = E_j(\{\mathbf{R}\})\,\Phi_j(\{\mathbf{r}\},\{\mathbf{R}\}) \tag{2.7}$$

is solved instantaneously for a given configuration of nuclei where $\{\mathbf{R}\}$ enters as a parameter. Its solution yields electronic wave functions Φ_j and a potential energy surface (PES) E_j for each electronic state j. The PES enters the nuclear Schrödinger equation

$$\begin{aligned}\hat{H}^{\mathrm{n}}_j\,\chi_{J,j}(\{\mathbf{R}\}) &= \left[\hat{T}^{\mathrm{n}} + \hat{W}^{\mathrm{nn}} + \varepsilon_j(\{\mathbf{R}\})\right]\,\chi_{J,j}(\{\mathbf{R}\}) \\ &= E^{\mathrm{n}}_{J,j}\,\chi_{J,j}(\{\mathbf{R}\})\end{aligned} \tag{2.8}$$

which determines the nuclear wave functions $\chi_{J,j}$ and yields a set of vibrational and rotational levels denoted by a collective index J for each electronic state j.

This is the standard Born-Oppenheimer picture of molecular dynamics with quantum mechanical electrons. The main goal of electronic structure theory is the solution of the electronic Schrödinger equation. Its solution determines all basic materials properties such as structure, vibrational frequencies, thermochemistry, electric and magnetic properties, and chemical reactivity.

2.2 Density Functional Theory

The electronic Schrödinger equation in Equation (2.7) is a quantum many-body problem, and solving it is a computationally demanding task. The presence of the electron-electron interaction term $\hat{W}^{\mathrm{ee}}$ in the electronic Hamiltonian causes this computational complexity. A direct computational solution of the electronic Schrödinger equation is possible. Post-Hartree-Fock methods such as the configuration interaction [31], coupled-cluster theory [6], multi-configurational self-consistent field approaches [30], or stochastic quantum Monte Carlo approaches [15] have been developed for this purpose. They have been applied successfully, but their computational cost is very high and their scaling with the number of electrons unfavorable. Therefore the direct methods are mainly applied to small systems and for the purpose of creating benchmark databases.

The vast majority of electronic structure calculations are DFT calculations. Due to its balance between accuracy and computational cost DFT has become the method of choice for solving the electronic Schrödinger equation both in quantum chemistry, condensed matter physics, and computational materials science [13].

2.2.1 Modern Density Functional Theory

Hohenberg-Kohn Theorem and the Universal Functional The variational principle in quantum mechanics states that the ground-state energy of the electronic Schrödinger equation is determined by a minimization over the electronic N^{e}-particle wavefunctions Φ that are antisymmetric, normalized, and have finite kinetic energy:

$$E = \min_{\Phi} \left(\langle \Phi | \hat{H}^{\mathrm{BO}} | \Phi \rangle \right) , \tag{2.9}$$

where we drop the electronic index j introduced in Equation (2.7) for notational simplicity.

Central to DFT is the Hohenberg-Kohn (HK) theorem [27] which states that the ground-state energy of the electronic Schrödinger equation can be found from

$$E = \min_{n} \left\{ F[n] + \int d^3r \, n(\mathbf{r}) \, v(\mathbf{r}) \right\} , \tag{2.10}$$

where F is a universal functional of the one-electron density n, because it is independent of the external potential v. The one-electron density is defined as

$$n(\mathbf{r}) = \int d\mathbf{r}_2 \cdots \int d\mathbf{r}_{N^{\mathrm{e}}} \; \Phi^*(\mathbf{r}, \mathbf{r}_2, \ldots, \mathbf{r}_{N^{\mathrm{e}}}) \, \Phi(\mathbf{r}, \mathbf{r}_2, \ldots, \mathbf{r}_{N^{\mathrm{e}}}) \tag{2.11}$$

in terms of the electronic N^{e}-particle wavefunctions Φ.

The universal functional F is defined by the constrained search procedure of Levy [42, 43] and Lieb [44, 45]:

$$\tilde{F}[n] = \min_{\Phi \to n} \langle \Psi | \hat{T}^{\mathrm{e}} + \hat{W}^{\mathrm{ee}} | \Phi \rangle \tag{2.12}$$

which follows from Equation (2.9) by writing the minimization in a two-step procedure, where the search is performed over all N^{e}-particle wavefunctions Φ that yield the one-electron density n.

Kohn-Sham Formalism of Modern Density Functional Theory Within the Kohn-Sham (KS) formalism we introduce a fictitious system of non-interacting electrons with the constraint that it yields the same one-electron density as obtained by solving the electronic Schrödinger equation. This is achieved by introducing an effective potential, the KS potential v_{S}, which formally represents all electron-electron interactions exactly within a mean-field description. The one-electron density is then constructed from

$$n(\mathbf{r}) = \sum_{j}^{N^{\mathrm{e}}} \phi_j^*(\mathbf{r}) \phi_j(\mathbf{r}) \tag{2.13}$$

where the KS orbitals ϕ_j are obtained by solving the KS equations

$$\left(-\frac{1}{2} \nabla_j^2 + v_{\mathrm{S}}(\mathbf{r}) \right) \phi_j(\mathbf{r}) = \varepsilon_j \, \phi_j(\mathbf{r}) \tag{2.14}$$

with ε_j denoting the corresponding KS orbital energies.

The KS potential is global, i.e., it is the same in all N^{e} KS equations. Despite its seemingly simple definition

$$v_{\mathrm{S}}(\mathbf{r}) = v_{\mathrm{ext}}(\mathbf{r}) + \frac{\delta E_{\mathrm{H}}[n]}{\delta n(\mathbf{r})} + \frac{\delta E_{\mathrm{XC}}[n]}{\delta n(\mathbf{r})}\,, \tag{2.15}$$

it is a complicated quantity, because it encodes all electron-electron interactions in a single-particle description. In the definition of the KS potential in Equation (2.15) we introduce two energy contributions. The Hartree energy

$$E_{\mathrm{H}}[n] = \frac{1}{2}\int d\mathbf{r} \int d\mathbf{r}'\, \frac{n(\mathbf{r}) - n(\mathbf{r}')}{|\mathbf{r} - \mathbf{r}'|} \tag{2.16}$$

representing the classical electrostatic energy of the electrons, and the exchange-correlation energy E_{XC} representing the remainder of the electron-electron interaction.

Whereas the exact expression of the Hartree energy as a density functional is known, an explicit and exact expression of E_{XC} in terms of a density functional is not known. In any pracitical DFT calculation an approximation to the exchange-correlation energy needs to be used.

2.2.2 Exchange-Correlation Approximations

Developing accurate approximations to the exchange-correlation energy is the central task in methods development within DFT.

Approximations developed for E_{XC} are important. They describe the bonding of nuclei to one another, and thus the exchange-correlation energy can be considered as nature's glue [35]. For example, neglecting exchange-correlation energy by imposing the approximation $E_{\mathrm{XC}} = 0$, as was originally done in solid state physics in the 1950's and 1960's, yields inaccurate results. We obtain lattice constants and bond lengths,about 10-20% larger than the exact, and binding energies of atoms much smaller than they actually are.

The exchange-correlation energy is commonly expressed as

$$E_{\mathrm{XC}}[n] = \int d\mathbf{r}\, n(\mathbf{r})\, \varepsilon_{\mathrm{XC}}[n](\mathbf{r})\,, \tag{2.17}$$

where $\varepsilon_{\mathrm{XC}}$ denotes the exchange-correlation energy density per particle.

In the following we give a very concise summary of the standard approximations in DFT. We refer to the standard literature for a more complete picture [32].

Local Density Approximation The earliest approximation to E_{XC} is the local density approximation (LDA) proposed alongside the KS equations [34]. The LDA provides the basis for many

methods that followed later, such as generalized gradient approximations (GGAs) [39, 52, 7, 41, 53, 49], meta-GGAs (MGGAs) [60], and hybrid functionals [49, 19, 1, 8, 57].

The LDA is expressed as

$$E_{\mathrm{XC}}^{\mathrm{LDA}}[n] = \int d\mathbf{r}\, n(\mathbf{r})\, \varepsilon_{\mathrm{XC}}^{\mathrm{LDA}}[n](\mathbf{r})\,, \tag{2.18}$$

where $\varepsilon_{\mathrm{XC}}^{\mathrm{LDA}} = -3/(2\pi)\left[3\pi^2 n(\mathbf{r})\right]^{1/3}$ is the exchange-correlation energy density per particle of the uniform electron gas. This is a Thomas-Fermi-like approximation [61, 21]. It is exact when the electron density is uniform and accurate when the density is slowly varying over space,

$$\frac{|\nabla n|}{n} \ll k_{\mathrm{F}} = (3\pi^2 n)^{1/3}\,, \quad \frac{|\nabla n|}{n} \ll k_{\mathrm{S}} = \frac{2}{\pi^{1/2}}(3\pi^2 n)^{1/6}\,, \tag{2.19}$$

where k_{F} is the Fermi wave vector, and k_{S} is the inverse of the Thomas-Fermi screening length.

Surprisingly LDA was found to predict lattice constants of solids, phonon frequencies, metal surface energies [38], and molecule geometries [28] very accurately.

Generalized Gradient Approximations The natural extension of the LDA is the inclusion of density gradients in the functional form of E_{XC}. Just adding the second-order density gradient expansion of the exchange-correlation energy did not yield sufficiently accurate results [40, 48]. Instead, a more complicated functional form, the generalized gradient approximation (GGA), was introduced. It is expressed as

$$E_{\mathrm{XC}}^{\mathrm{GGA}}[n] = \int d\mathbf{r}\, n(\mathbf{r})\, \varepsilon_{\mathrm{XC}}^{\mathrm{GGA}}[n, |\nabla n|](\mathbf{r}) \tag{2.20}$$

where $\varepsilon_{\mathrm{XC}}^{\mathrm{GGA}}$ includes higher order derivatives such as $|\nabla n|^4, |\nabla n|^6, |\nabla n|^8$, etc. [39]. More commonly the GGA is expressed as

$$E_{\mathrm{XC}}^{\mathrm{GGA}}[n] = \int d\mathbf{r}\, F_{\mathrm{XC}}[n, |\nabla n|](\mathbf{r})\, n(\mathbf{r})\, \varepsilon_{\mathrm{X}}^{\mathrm{LDA}}[n](\mathbf{r}) \tag{2.21}$$

in terms of an enhancement factor, F_{XC}, over the local exchange energy density per particle $\varepsilon_{\mathrm{X}}^{\mathrm{LDA}}$.

Suitable forms for F_{XC} have been developed and parametrized as analytic functions by fitting to reference systems like atoms [7] or to exact constraints on the exchange-correlation energy functional [39, 52, 53, 49]. Despite significant improvements over the LDA, the functional form of the GGA is still too limited to simultaneously yield accurate bond lengths and accurate binding energies.

Beyond Generalized Gradient Approximations The logical step to go beyond GGAs is to include the kinetic energy density of the KS system, τ_{S}, in the construction of the E_{XC}. This class of exchange-correlation functional is called MGGA. Inclusion of the KS kinetic energy density

enables the functional to detect various regimes of electron-electron interaction, such as single, metallic and noncovalent bonds. The MGGA is expressed as

$$E_{\mathrm{XC}}^{\mathrm{MGGA}}[n] = \int d\mathbf{r}\, n(\mathbf{r})\, \varepsilon_{\mathrm{XC}}^{\mathrm{MGGA}}[n, |\nabla n|, \tau_{\mathrm{S}}](\mathbf{r}) \; . \tag{2.22}$$

MGGAs depend explicitly on the density n, its gradients and on the KS orbitals via τ_{S}. Nevertheless, they are density functionals, because ϕ_i are functionals of the KS potential, v_{S}.

In earlier developments of MGGAs the Laplacian of the density, $\nabla^2 n$, was deployed [55, 18, 10, 22, 23]. More recently the KS kinetic energy density, $\tau_{\mathrm{S}}[n]$, has been used in their construction [62, 36, 50, 20, 60, 65, 51, 16, 58, 59].

Other approaches beyond GGAs and MGGAs include approximations that explicitly depend on the occupied KS orbitals in a non-local way such as the exact exchange functional, hybrid functionals [49, 19, 1, 8, 57], and functionals that depend also on unoccupied KS orbitals and on KS orbital energies such as the random-phase-approximation [40].

The computational evaluation of MGGAs as defined in Equation (2.22) is computationally feasible, because only a single three-dimensional integral over all space needs to be performed. However, exchange-correlation approximations beyond the level of MGGAs are computationally much more expensive. For example many hybrid functionals involve double integrals or even multiple integrals over three-dimensional space which makes these approaches much more costly. This adversely affects the system sizes that can be achieved even using high-performance computing resources.

The exchange-correlation functional we develop in this report falls under the category of MGGAs. However, it differs significantly from other MGGAs by its use of the subsystem functional formalism and the electron localization function (ELF) [9]. Both concepts will be introduced in Section 3.3 and in Appendix A. They enable us to include confinement physics into the construction of the exchange-correlation functional.

2.3 The Jellium Surface Reference System

The jellium model, also called the uniform electron gas or the homogeneous electron gas, is the cornerstone for the construction of exchange-correlation functionals. Highly accurate quantum Monte-Carlo (QMC) calculations of the exchange-correlation energy[15, 14] form the basis of the LDA[63, 47, 53] which is a parametrization of the QMC results in terms of a local density functional.

While the jellium model serves as a suitable representation of the bulk physics, the jellium surface model is a paradigm for representing the surface physics of electronic correlation effects [37, 64, 54]. The jellium surface is defined by a jellium slab of thickness d aligned along

the z axis. Its external potential is given by

$$v(z) = \begin{cases} \bar{n} & -d/2 \leq z \leq d/2\,, \\ 0 & else\,, \end{cases} \tag{2.23}$$

where $\bar{n}$ denotes a background of positive charge. The jellium surface energy is given by

$$\sigma = \sigma_{\mathrm{S}} + \sigma_{\mathrm{H}} + \sigma_{\mathrm{XC}}\,, \tag{2.24}$$

where

$$\sigma_{\mathrm{S}} = \frac{1}{4\pi}\sum_{i=1}^{N}(E_{\mathrm{F}}^2 - \varepsilon_i^2) - \frac{k_{\mathrm{F}}^5 d}{20\pi^2} - \int_0^\infty dz\, n(z)\,[v_{\mathrm{S}}(z) - v_{\mathrm{S}}(0)] \tag{2.25}$$

is the kinetic surface energy of non-interacting electrons,

$$\sigma_{\mathrm{H}} = \frac{1}{2}\int_0^\infty dz\ [n(z) - n_+(z)]\, v_{\mathrm{H}}(z) \tag{2.26}$$

is the electrostatic surface energy, and

$$\sigma_{\mathrm{XC}} = \int_0^\infty dz\, n(z)\left\{\varepsilon_{\mathrm{XC}}[n](\mathbf{r}) - \varepsilon_{\mathrm{XC}}^{\mathrm{LDA}}[\bar{n}]\right\} \tag{2.27}$$

is the exchange-correlation surface energy. The quantities E_{F} denote the Fermi level, $k_{\mathrm{F}} = (3\pi^2\bar{n})^{1/3}$ the Fermi momentum, v_{H} the electrostatic potential, and $v_{\mathrm{S}} = v_{\mathrm{H}} + v_{\mathrm{XC}}$ the KS potential.

The jellium surface energies computed within the random-phase approximation are considered as the most accurate [64, 54]. The corresponding exchange, correlation, and exchange-correlation surface energies are given in Table 2.1 for several values of the Wigner-Seitz radius $r_{\mathrm{S}} = [3/(4\pi n)]^{1/3}$. The Wigner-Seitz is a dimensionless radius of a sphere that contains the charge of one electron and is commonly used as a measure to characterize the density of a system. We will use these jellium surface energies as reference values for developing our exchange-correlation approximation.

Table 2.1. Exchange, correlation, and exchange-correlation surface energies of the jellium surface reference system.

r_S	σ_X	σ_C	σ_{XC}
2.00	2624	789	3413
2.07	2296	719	3015
2.30	1521	539	2060
2.66	854	360	1214
3.00	526	255	781
3.28	364	199	563
4.00	157	111	268

Chapter 3

Construction and Assessment of the Exchange-Correlation Functional Capturing Bulk, Surface, and Confinement Physics

3.1 Exchange Functional for Confinement Physics

In our construction of an exchange functional we use the harmonic oscillator gas (HOG) as a reference system in order to capture confinement physics. We first derive analytical results of the HOG and subsequently parameterize them to obtain an accurate exchange functional.

The Harmonic Oscillator Gas Reference System The HOG reference system consists of non-interacting fermions within an three-dimensional potential which is only confined along the z axis by a parabolic potential

$$v_{\text{eff}}(z) = \frac{\omega^2}{2} z^2 \,, \tag{3.1}$$

where ω denotes the frequency of the harmonic oscillator. The potential is not confined along the x and y axes. The solution of the KS equations

$$\left(-\frac{1}{2}\nabla^2 + v_{\text{eff}}(z) \right) \psi_\kappa(\mathbf{r}) = \varepsilon_\kappa \, \psi_\kappa(\mathbf{r}) \tag{3.2}$$

yields

$$\psi_\kappa(\mathbf{r}) = \frac{\exp[i(k_x x + k_y y)]}{L_x L_y} \, \phi_j(z) \,, \tag{3.3}$$

where $\kappa = (k_x, k_y, j)$, (k_x, k_y) denotes the in-plane wave vectors which satisfy $k_i L_i = 2\pi n_i$ with $i = x, y$, and $n_i \in \mathbb{I}$. The factorization of the solutions ψ_κ reflects the free electrons along the x and y axes by the plane-wave prefactor and the confined electrons along the z axis by the KS orbitals

$\phi_j(z)$. They are obtained by solving the KS equations

$$\left(-\frac{1}{2}\frac{d^2}{d\bar{z}^2}+v_{\text{eff}}(\bar{z})\right)\phi_j(\bar{z})=l^2\varepsilon_j\,\phi_j(\bar{z})\,, \tag{3.4}$$

in a dimensionless coordinate $\bar{z}=x/l$ with a scale parameter $l=\sqrt{1/\omega}$. The analytical solutions are

$$\phi_j(\bar{z})=\left(\frac{1}{2^j\,j!\,l\sqrt{\pi}}\right)^{1/2}H_j(\bar{z})\,\exp(-\bar{z}^2/2) \tag{3.5}$$

with the corresponding eigenvalues

$$\varepsilon_j=\frac{1}{l^2}\left(j+\frac{1}{2}\right), \tag{3.6}$$

where $H_j(\bar{z})$ denotes the Hermite polynomials.

The dimensionless density of the HOG is then expressed as

$$[l^3\,n(\bar{z})]=\frac{1}{\pi^{3/2}}\sum_{j=0}^{N}\frac{1}{2^j\,j!}H_j^2(\bar{z})\,(\alpha-j)\,\exp(-\bar{z}^2)\,, \tag{3.7}$$

where $\alpha\in\mathbb{R}$ determines the degree of confinement in the HOG reference system. It is defined in terms of the chemical potential

$$\mu=\frac{\alpha+\frac{1}{2}}{l^2}\,, \tag{3.8}$$

where $\lfloor\alpha\rfloor=N^{\text{e}}$ determines the highest occupied KS level in the confined parabolic potential.

The dimensionless exchange energy density per particle of the HOG is expressed as

$$[l^3\,\varepsilon_{\text{X}}(\bar{z})]=-\frac{1}{2\pi^2[l^3\,n(\bar{z})]}\int d\bar{z}\sum_{j=0}^{N^{\text{e}}}\sum_{k=0}^{N^{\text{e}}}\frac{\exp[-(\bar{z}^2+\bar{z}'^2)]}{2^j\,j!\,2^k\,k!}H_j(\bar{z})\,H_j(\bar{z}')\,H_k(\bar{z})\,H_k(\bar{z}') \tag{3.9}$$

$$\times\frac{I\left(\sqrt{2(\alpha-j)}|\bar{z}-\bar{z}'|,\sqrt{2(\alpha-k)}|\bar{z}-\bar{z}'|\right)}{|\bar{z}-\bar{z}'|^3}\,, \tag{3.10}$$

where we introduced a short-hand notation

$$I(\alpha,\beta)=\alpha\,\beta\int_0^\infty dt\,\frac{J_1(\alpha\,t)\,J_1(\beta\,t)}{t\sqrt{1+t^2}} \tag{3.11}$$

with $J_1(z)$ denoting the Bessel function of first kind.

Construction of the HOG Exchange Functional As introduced in Equation (2.20) we express the exchange energy density per particle as

$$\varepsilon_{\mathrm{X}}^{\mathrm{conf}}[n](\mathbf{r}) = \varepsilon_{\mathrm{X}}^{\mathrm{HOG}}[n](\mathbf{r}) = \varepsilon_{\mathrm{X}}^{\mathrm{LDA}}[n,|\nabla n|,\mathrm{ELF}](\mathbf{r})\, F_{\mathrm{X}}^{\mathrm{HOG}}[n,|\nabla n|,\mathrm{ELF}](\mathbf{r}) \tag{3.12}$$

in terms of an enhancement factor $F_{\mathrm{X}}^{\mathrm{HOG}}$ which includes confinement physics. We follow a similar approach to the parametrization of the enhancement factor as in the AM05 functional[4]. We derive analytical expressions for the exact exchange energy of Equation (3.9) both in the limit of small and large $\bar{z}$. By interpolating between the limits we obtain a functional form only in terms of the density, its gradient, and the ELF [9]:

$$F_{\mathrm{X}}^{\mathrm{HOG}}[n,|\nabla n|,\mathrm{ELF}](\mathbf{r}) = \frac{[l\,\varepsilon_{\mathrm{X}}[n,|\nabla n|,\mathrm{ELF}](\mathbf{r})]^{\mathrm{HOG}}}{[l\,\varepsilon_{\mathrm{X}}[n,|\nabla n|,\mathrm{ELF}](\mathbf{r})]^{\mathrm{LDA}}}\,, \tag{3.13}$$

where $[l\,\varepsilon_{\mathrm{X}}[n,|\nabla n|,\mathrm{ELF}](\mathbf{r})]^{\mathrm{LDA}}$ and $[l\,\varepsilon_{\mathrm{X}}[n,|\nabla n|,\mathrm{ELF}](\mathbf{r})]^{\mathrm{HOG}}$ are parameterizations of the dimensionless exchange energy density per particle of the LDA and the HOG reference system given in Equation (3.9). Definitions and details of the derivation of the HOG exchange functional are given in Appendix A.

Assessment of the HOG Exchange Functional in the Jellium Surface Reference System To assess the accuracy and transferability of the HOG exchange functional we apply it to the jellium surface reference system introduced in Section 2.3. We evaluate the HOG jellium surface densities along with several standard exchange functionals such as LDA, PBE, and AM05. The corresponding exchange surface energies are given in Table 3.3. The resulting mean absolute relative errors are 24.8% for LDA, 11.0% for PBE, 15.4% for AM05, and 4.8% for HOG.

Having demonstrated its accuracy we will subsequently use the HOG exchange functional as the exchange component for capturing confinement physics within the subsystem functional formalism. This will be discussed in Section 3.3.

Table 3.1. Comparison of exchange surface energies obtained from standard functionals (LDA, PBE, AM05) and the HOG exchange functional $\varepsilon_{\mathrm{X}}^{\mathrm{HOG}}$ with the jellium surface reference system.

r_{S}	$\sigma_{\mathrm{X}}^{\mathrm{LDA}}$	$\sigma_{\mathrm{X}}^{\mathrm{PBE}}$	$\sigma_{\mathrm{X}}^{\mathrm{AM05}}$	$\sigma_{\mathrm{X}}^{\mathrm{HOG}}$	σ_{X}
2.00	3036.33	2436.31	2895.98	2586.68	2624
2.07	2673.31	2125.31	2543.50	2258.26	2296
2.30	1808.23	1393.45	1706.30	1484.54	1521
2.66	1050.90	769.00	978.36	822.51	854
3.00	668.43	463.90	613.93	497.71	526
3.28	476.57	315.46	432.59	339.16	364
4.00	222.16	127.56	195.02	137.85	157
MARE	24.8%	11.0%	15.4%	4.8%	–

3.2 Correlation Functional for Confinement Physics

Construction of a Correlation Functional Compatible with the HOG Exchange Functional
We construct a correlation functional compatible with the HOG exchange functional by parametrizing the jellium surface correlation energy. Our method of construction assumes that the errors in the HOG exchange functional are negligible as demonstrated in Table 3.3. The parametrization of the HOG correlation functional is performed using the following functional form:

$$\varepsilon_{\mathrm{C}}^{\mathrm{HOG}}[n,|\nabla n|](\mathbf{r}) = \varepsilon_{\mathrm{C}}^{\mathrm{LDA}}[n](\mathbf{r})\left\{X_{\mathrm{surf},1}(\mathbf{r};\eta_1) + [1 - X_{\mathrm{surf},1}(\mathbf{r};\eta_1)](\gamma_1 + \gamma_2 r_{\mathrm{S}})\right\}, \tag{3.14}$$

where

$$X_{\mathrm{surf},1}(\mathbf{r};\eta_1) = 1 - \frac{\eta_1 s^2(\mathbf{r})}{1 + \eta_1 s^2(\mathbf{r})} \tag{3.15}$$

is an interpolation index which discriminates between the bulk and surface region within the jellium reference system, $s(\mathbf{r}) = |\nabla n(\mathbf{r})|/[2(3\pi^2)^{1/3} n^{4/3}(\mathbf{r})]$ denotes the reduced density gradient, and η_1, γ_1, and γ_2 are parameters. The given functional form of $\varepsilon_{\mathrm{C}}^{\mathrm{HOG}}$ is a scaled version of the LDA correlation functional. The interpolation index $X_{\mathrm{surf},1}$ is defined such that the HOG correlation functional reduces correctly to the LDA correlation functional in the bulk region ($s = 0$). In the surface region when s has a finite value, the LDA correlation functional is enhanced by the scale factor given in Equation (3.14). The functional form of $\varepsilon_{\mathrm{C}}^{\mathrm{HOG}}$ is similar to the correlation component of the AM05 functional [4]. However, it has an additional parameter, γ_2, which enables us to parametrize the jellium surface correlation energy more accurately and provides more flexibility for a better compatibility with the HOG exchange functional.

The parameters η_1, γ_1, and γ_2 are determined by a nonlinear fit to the jellium surface correlation energies given in Table 2.1. We obtain $\eta_1 = -1.48051$, $\gamma_1 = 0.0224407$, and $\gamma_2 = 0.0367228$.

Assessment of the HOG Correlation Functional in the Jellium Surface Reference System
We assess the accuracy of the HOG correlation functional by applying it to the jellium surface reference system. We evaluate $\varepsilon_{\mathrm{C}}^{\mathrm{HOG}}$ as well as standard correlation functionals such LDA in the Perdew-Wang parametrization [53], PBE, and AM05 on the jellium surface densities. The resulting correlation surface energies are given in Table 3.2. The mean absolute relative errors are 62.0% for LDA, 6.9% for PBE, 3.9% for AM05, and 0.2% for our HOG correlation functional.

While many standard exchange-correlation functionals such as LDA, PBE, and AM05 rely on error cancellation of the respective exchange and correlation energy contributions, we develop an exchange-correlation functional which is accurate in each of these energy components, and hence, does not rely on the cancellation of errors. We achieve this by using the HOG exchange functional and the compatible HOG correlation functional within the subsystem functional formalism which is discussed in Section 3.3.

Table 3.2. Comparison of correlation surface energies obtained from standard functionals (LDA, PBE, AM05) and our HOG functional $\varepsilon_{\mathrm{C}}^{\mathrm{HOG}}$ with the jellium surface reference system.

r_{S}	$\sigma_{\mathrm{C}}^{\mathrm{LDA}}$	$\sigma_{\mathrm{C}}^{\mathrm{PBE}}$	$\sigma_{\mathrm{C}}^{\mathrm{AM05}}$	$\sigma_{\mathrm{C}}^{\mathrm{HOG}}$	σ_{C}
2.00	317.25	827.28	780.12	789.32	789
2.07	286.81	753.75	712.53	718.79	719
2.30	210.29	566.52	539.71	538.60	539
2.66	136.45	381.46	367.56	359.78	360
3.00	94.97	274.61	267.27	256.24	255
3.28	72.34	214.99	210.88	198.44	199
4.00	38.99	124.30	124.24	110.78	111
MARE	62.0%	6.9%	3.9%	0.2%	–

3.3 Construction of the Exchange-Correlation Functional within the Subsystem Functional Formalism

We construct an exchange-correlation functional which is accurate in the relevant physical regimes capturing bulk physics, surface physics, and confinement physics by combining the individual components $\varepsilon_{\mathrm{XC}}^{bulk}$, $\varepsilon_{\mathrm{XC}}^{surf}$, and $\varepsilon_{\mathrm{XC}}^{conf}$ with the aid of the subsystem functional formalism.

We construct our general subsystem exchange-correlation functional by expressing the abstract sum in Equation (3.16) in terms of an interpolation. The challenge is to find accurate interpolation indices which will correctly tune the appropriate contributions from the separate physical regimes.

3.3.1 The Subsystem Functional Formalism

Based on the principle of near-sightedness [33], the subsystem functional formalism is a suitable method to construct an exchange-correlation functional which incorporates the characteristic physics of different regimes. Within the subsystem functional formalism the total exchange-correlation energy defined in Equation (2.17) is divided into contributions from different subsystems

$$E_{\mathrm{XC}} = \sum_j \int_{\Omega_j} d\mathbf{r}_j \, n(\mathbf{r}) \, \varepsilon_{\mathrm{XC}}^j[n](\mathbf{r}) \,, \tag{3.16}$$

where $\varepsilon_{\mathrm{XC}}^j$ denotes the exchange-correlation energy density per particle and Ω_j the volume of subsystem j.

The overall accuracy of a subsystem functional relies on the accuracy of the particular subsytem exchange-correlation functionals. Bulk physics in the interior of a material is accurately

represented by the LDA

$$\varepsilon_{\mathrm{XC}}^{bulk}[n](\mathbf{r}) = \varepsilon_{\mathrm{XC}}^{\mathrm{LDA}}[n](\mathbf{r}) \tag{3.17}$$

which uses the uniform electron gas as a reference system. Surface physics is accurately represented by the AM05 functional

$$\varepsilon_{\mathrm{XC}}^{surf}[n](\mathbf{r}) = \varepsilon_{\mathrm{XC}}^{\mathrm{AM05}}[n,|\nabla n|](\mathbf{r}) \tag{3.18}$$

which uses the Airy gas as a reference system. Here we develop an exchange-correlation functional which accurately represents confinement physics

$$\varepsilon_{\mathrm{XC}}^{conf}[n](\mathbf{r}) = \varepsilon_{\mathrm{XC}}^{\mathrm{HOG}}[n,|\nabla n|,\mathrm{ELF}](\mathbf{r}) \tag{3.19}$$

which is a combination of the HOG exchange functional based on the HOG reference system and the HOG correlation functional based on the jellium surface reference system.

3.3.2 Subsystem Exchange Functional Capturing Bulk, Surface, and Confinement Physics

Construction of the Subsystem BSC Exchange Functional We construct an exchange functional, $\varepsilon_{\mathrm{X}}^{\mathrm{BSC}}$, which is accurate in the bulk, surface, and confinement regions, hence the acronym BSC.

The key quantity which we use to distinguish between physical regimes is the ELF. Its behavior in the jellium surface reference system is illustrated in Figure 3.1 for several values of the Wigner-Seitz radius. Its numerical value gives a clear indication of the type of physics present in different regions of space. For example, in regions of space where $\mathrm{ELF}(\mathbf{r}) = 0.5$ the system is dominated by bulk physics, where $\mathrm{ELF}(\mathbf{r}) < 0.5$ by surface physics, and where $\mathrm{ELF}(\mathbf{r}) > 0.5$ by confinement physics.

In order to construct the BSC exchange functional and with the aid of the ELF, we define the interpolation index

$$X_{\mathrm{ELF}}(\mathbf{r};\eta_2) = 1 - \frac{\eta_2\,[\mathrm{ELF}(\mathbf{r}) - 1/2]^4}{1 + \eta_2\,[\mathrm{ELF}(\mathbf{r}) - 1/2]^4} \tag{3.20}$$

along with an auxiliary interpolation index for the surface region

$$X_{\mathrm{surf},2}(\mathbf{r};\eta_3) = \frac{2}{1 + e^{2\,\eta_3\,s^2(\mathbf{r})}}\,, \tag{3.21}$$

where η_2 and η_3 are parameters. X_{ELF} and $X_{\mathrm{surf},2}$ enable us to represent the sum over subsystems in Equation (3.16) in terms of an interpolation.

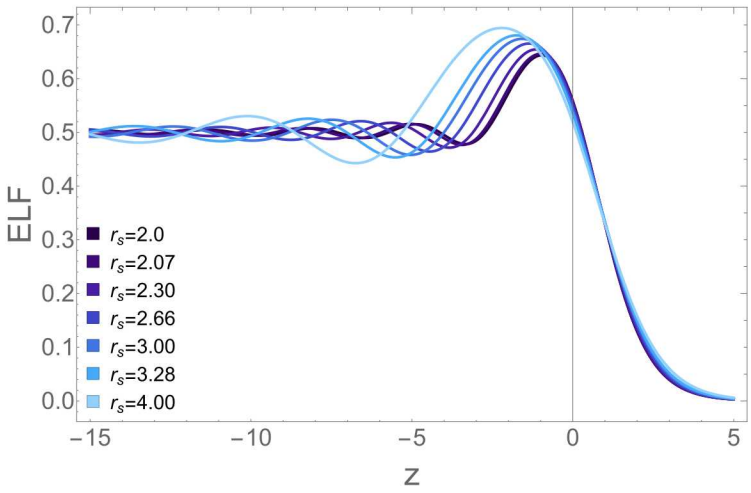

Figure 3.1. Illustration of the ELF in the jellium surface reference system for several values of the Wigner-Seitz radius.

Hence, the subsystem BSC exchange functional is expressed as

$$\begin{aligned}\varepsilon_{\mathrm{X}}^{\mathrm{BSC}} = \varepsilon_{\mathrm{X}}^{\mathrm{surf}} \{1 + [X_{\mathrm{ELF}} - 1][1 + X_{\mathrm{ELF}}(X_{\mathrm{surf},2} - 1)]X_{\mathrm{surf},2}\} \\ + \varepsilon_{\mathrm{X}}^{\mathrm{conf}} \{1 + X_{\mathrm{ELF}}[X_{\mathrm{surf},2} - 1]\}[1 - X_{\mathrm{ELF}}X_{\mathrm{surf},2}],\end{aligned} \tag{3.22}$$

where the surface term $\varepsilon_{\mathrm{X}}^{\mathrm{surf}}$ becomes the bulk term $\varepsilon_{\mathrm{X}}^{\mathrm{bulk}}$ in the limit of vanishing density gradient when $s^2(\mathbf{r}) \to 0$.

We determine the values of the parameters η_2 and η_3 by tuning the relevance of the interpolation indices in the bulk, surface, and confinement regions. This is illustrated in Figure 3.2, where we plot the exchange surface energy density per particle for the LDA (blue), PBE (green), AM05 (red), and BSC (black) exchange functionals. From the figure we infer that the PBE functional underestimates the surface exchange energy, whereas the AM05 functional overestimates it. The optimum values for the parameters in the BSC exchange functional are $\eta_2 = 10^5$ and $\eta_3 = 1.6875$ and for which we obtain a balanced approximation resulting in an improvement upon both the PBE and AM05 functionals, in particular in the region $(-2 \leq z \leq 3)$ relevant for confinement physics where $\mathrm{ELF}(\mathbf{r}) > 0.5$. In order to avoid numerical instabilities due to the Fermi-Dirac-like broadening in Equation (3.21) we will explore rational approximations [46].

Assessment of the BSC Exchange Functional in the Jellium Surface Reference System We assess the accuracy of our subsystem BSC exchange functional by applying it to the jellium surface reference system and comparing it to the standard exchange functionals LDA, PBE, and AM05. The resulting surface exchange energies are given in Table 3.3. The resulting mean absolute relative error of the subsystem BSC exchange functional is 0.8% which is significantly smaller than the error of the standard functionals. In addition, we include the HOG exchange functional derived in Equation (3.12) in the comparison. As expected, the subsystem BSC exchange functional

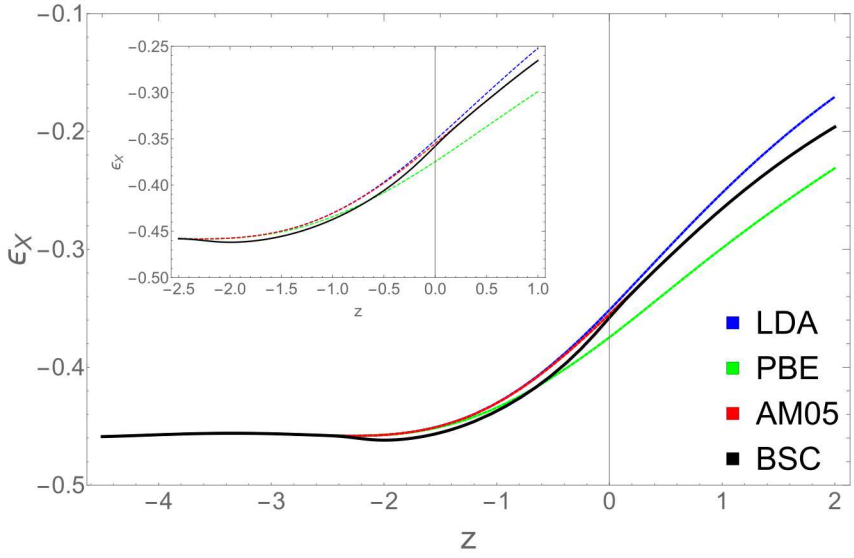

Figure 3.2. Exchange surface energy densities per particle, ε_{X}, at $r_{\mathrm{s}} = 2.0$ for the LDA (blue), PBE (green), AM05 (red), and BSC (black) exchange functionals. The range illustrated is roughly the region of space where confinement physics is relevant (see Figure 3.1).

is more accurate. While both the HOG and the BSC exchange functionals are identical in their representation of confinement physics, the BSC functional is more accurate in the other physical regimes due to the interpolation within the subsystem functional formalism.

3.3.3 Subsystem Exchange-Correlation Functional Capturing Bulk, Surface, and Confinement Physics

Construction of the Subsystem BSC Exchange-Correlation Functional We construct the subsystem BSC exchange-correlation functional, $\varepsilon_{\mathrm{XC}}^{\mathrm{BSC}}$, by combining the BSC exchange functional with the HOG correlation functional developed in Equation (3.14). This yields

$$\varepsilon_{\mathrm{XC}}^{\mathrm{BSC}}[n,|\nabla n|,\mathrm{ELF}](\mathbf{r}) = \varepsilon_{\mathrm{X}}^{\mathrm{BSC}}[n,|\nabla n|,\mathrm{ELF}](\mathbf{r}) + \varepsilon_{\mathrm{C}}^{\mathrm{HOG}}[n,|\nabla n|](\mathbf{r}), \tag{3.23}$$

where the parameters η_1, η_2, η_3, γ_1, and γ_2 take the optimized values for the exchange and correlation contributions within the jellium surface reference system determined in Section 3.2 and Section 3.3.2.

Assessment of the BSC Exchange-Correlation Functional in the Jellium Surface Reference System We assess the accuracy of the BSC exchange-correlation functional by applying it to

Table 3.3. Comparison of exchange surface energies obtained from standard functionals (LDA, PBE, AM05), the HOG functional, and the BSC functional with the jellium surface reference system.

r_s	σ_x^{LDA}	σ_x^{PBE}	σ_x^{AM05}	σ_x^{HOG}	σ_x^{BSC}	σ_x
2.00	3036.33	2436.31	2895.98	2586.68	2637.13	2624
2.07	2673.31	2125.31	2543.50	2258.26	2307.14	2296
2.30	1808.23	1393.45	1706.30	1484.54	1527.50	1521
2.66	1050.90	769.00	978.36	822.51	856.28	854
3.00	668.43	463.90	613.93	497.71	524.61	526
3.28	476.57	315.46	432.59	339.16	361.47	364
4.00	222.16	127.56	195.02	137.85	152.14	157
MARE	24.8%	11.0%	15.4%	4.8%	0.8%	–

Table 3.4. Comparison of exchange-correlation surface energies obtained from standard functionals (LDA, PBE, AM05) and the BSC functional ε_{xc}^{BSC} with the jellium surface reference system.

r_s	σ_{xc}^{LDA}	σ_{xc}^{PBE}	σ_{xc}^{AM05}	σ_{xc}^{BSC}	σ_{xc}
2.00	3354	3263.58	3413.95	3426.68	3413
2.07	2961	2879.06	3014.59	3026.14	3015
2.30	2019	1959.97	2058.40	2066.13	2060
2.66	1188	1150.46	1213.52	1216.06	1214
3.00	764	738.51	782.02	780.78	781
3.28	549	530.45	563.44	559.91	563
4.00	261	251.86	269.63	262.93	268
MARE	2.0%	5.2%	0.1%	0.5%	–

the jellium surface reference system. We evaluate ε_{xc}^{BSC} as well as standard exchange-correlation functionals such LDA, PBE, and AM05 on the jellium surface densities. The resulting exchange-correlation surface energies are given in Table 3.4. The resulting mean absolute relative errors are 2% for LDA, 5.2% for PBE, 0.1% for AM05, and 0.5% for the BSC exchange-correlation functional. As expected, the AM05 functional yields the most accurate results, because the jellium surface is its reference system. The BSC functional is comparable in accuracy and additionally has the ability to capture confinement physics. A further discussion of these results is given in Section 4.

Chapter 4

Conclusion

4.1 Summary

In this report we have outlined the construction of a single exchange-correlation functional, the BSC functional, which captures bulk, surface, and confinement physics. The core of our construction relies on the subsystem functional formalism which together with an interpolation index based on the ELF enabled us to combine accurate functionals adapted to these different physical regimes into a single exchange-correlation functional. We expect that the inclusion of the HOG functional as the component for capturing confinement physics should yield significantly more accurate energetics of materials containing f and d electrons than existing semilocal GGA and MGGA functionals.

We want to point out that the performance of the BSC functional is comparable to the AM05 functional for the jellium surface reference system. However, the current form of the BSC functional has not been finalized yet, it will be further improved. We expect improvements in the accuracy of the BSC functional by (1) by performing a more systematic optimization of the parameters and (2) by implementing other functional forms of the interpolation indices. Despite its comparable performance to AM05 in the jellium surface reference system, the relevant assessment of the BSC functional will be the materials tests discussed in the next section.

4.2 Future Work

The BSC exchange-correlation functional we constructed is a prototype of an exchange-correlation functional with the aim to capture the physics of d and f electrons. Several developments are currently in progress.

The next step is to implement the BSC exchange-correlation functional into an open-source electronic structure code such as Quantum ESPRESSO [26, 25] and ELK [17]. This will enable us to assess the accuracy BSC exchange-correlation functional for materials containing d and f electrons.

We will first begin with tests of the BSC exchange-correlation functional on simple mate-

rials such as crystalline silicon and aluminum. Then we will assess the accuracy of the BSC functional in capturing confinement physics by computing the electronic properties of crystalline cobalt, nickel, and copper oxide. Crystalline copper oxide is a particularly useful test system, because it exhibits the same exchange-correlation physics as actinide systems, but without any relativistic effects. Therefore it provides a pure testing ground for the BSC exchange-correlation functional.

Once these initial assessments of the BSC functionals have been completed we intend to perform tests on a larger scale. In the course of this project we have generated a representative database of binary transition metal compounds (metals containing two different types of transition metal ions) for benchmarking exchange-correlation functionals (such as LDA, PBE, PW91, PBEsol, RTPSS, M06-L, and AM05) with respect to formation energy differences, ground state structures, lattice and elastic constant. This database will serve as a useful reference to assess the accuracy of our BSC functional.

Parallel to testing the BSC exchange-correlation functional, we will continue to improve its accuracy by refining its parameters and exploring different functional forms for the interpolation between the subsystems. For example, in its current form we have taken optimized parameters only for the separate subsystems. We expect improvements by performing a more systematic optimization of its parameters by considering the entire functional form within the jellium surface reference system. Furthermore, we will explore other functional forms for the interpolation index which will likely further improve the accuracy. In particular, the materials tests will indicate where further modifications of the functional form might be necessary.

References

[1] C. Adamo and V. Barone. Toward reliable density functional methods without adjustable parameters: The pbe0 model. *J. Chem. Phys.*, 110:6158, 1999.

[2] V. I. Anisimov, I. V. Solovyev, M. A. Korotin, M. T. Czyżyk, and G. A. Sawatzky. Density-functional theory and nio photoemission spectra. *Phys. Rev. B*, 48:16929–16934, Dec 1993.

[3] Vladimir I. Anisimov, Jan Zaanen, and Ole K. Andersen. Band theory and mott insulators: Hubbard u instead of stoner i. *Phys. Rev. B*, 44:943–954, Jul 1991.

[4] R. Armiento and A. E. Mattsson. Functional designed to include surface effects in self-consistent density functional theory. *Phys. Rev. B*, 72:085108, Aug 2005.

[5] Ferdi Aryasetiawan and Silke Biermann. Generalized hedin equations and gw approximation for quantum many-body systems with spin-dependent interactions. *Journal of Physics: Condensed Matter*, 21(6):064232, 2009.

[6] Rodney J. Bartlett and Monika Musiał. Coupled-cluster theory in quantum chemistry. *Rev. Mod. Phys.*, 79:291–352, Feb 2007.

[7] A. D. Becke. Density-functional exchange-energy approximation with correct asymptotic behavior. *Phys. Rev. A*, 38(6):3098–3100, Sep 1988.

[8] A. D. Becke. Density-functional thermochemistry. iii. the role of exact exchange. *J. Chem. Phys.*, 98(7):5648–5652, 1993.

[9] A. D. Becke and K. E. Edgecombe. A simple measure of electron localization in atomic and molecular systems. *The Journal of Chemical Physics*, 92(9):5397–5403, 1990.

[10] Axel D. Becke. A new inhomogeneity parameter in density-functional theory. *J. Chem. Phys.*, 109:2092–2098, 1998.

[11] M. Born and K. Huang. *Dynamical Theory of Crystall Lattices*. Oxford University Press, New York, 1954.

[12] M. Born and R. Oppenheimer. Zur quantentheorie der molekeln. *Ann. Phys.*, 389(20):457–484, 1927.

[13] Kieron Burke. Perspective on density functional theory. *J. Chem. Phys.*, 136(15):–, 2012.

[14] D. M. Ceperley. Path integrals in the theory of condensed helium. *Rev. Mod. Phys.*, 67:279–355, Apr 1995.

[15] D. M. Ceperley and B. J. Alder. Ground state of the electron gas by a stochastic method. *Phys. Rev. Lett.*, 45:566–569, Aug 1980.

[16] Jorge M. del Campo, José L. Gázquez, S.B. Trickey, and Alberto Vela. A new meta-GGA exchange functional based on an improved constraint-based GGA. *Chem. Phys. Lett.*, 543:179–183, 2012.

[17] Kay Dewhurst, Sangeeta Sharma, Lars Nordström, Francesco Cricchio, Oscar Grånäs, Hardy Gross, Claudia Ambrosch-Draxl, Clas Persson, Fredrik Bultmark, Christian Brouder, Rickard Armiento, Andrew Chizmeshya, Per Anderson, Igor Nekrasov, Frank Wagner, Fateh Kalarasse, Jürgen Spitaler, Stefano Pittalis, Nektarios Lathiotakis, Tobias Burnus, Stephan Sagmeister, Christian Meisenbichler, Sébastien Lebègue, Yigang Zhang, Fritz Körmann, Alexey Baranov, Anton Kozhevnikov, Shigeru Suehara, Frank Essenberger, Antonio Sanna, Tyrel McQueen, Tim Baldsiefen, Marty Blaber, Anton Filanovich, Torbjörn Björkman, Martin Stankovski, Jerzy Goraus, Markus Meinert, Daniel Rohr, Vladimir Nazarov, Kevin Krieger, Arkardy Davydov, Florian Eich, Aldo Romero Castro, Koichi Kitahara, James Glasbrenner, Konrad Bussmann, Igor Mazin, Matthieu Verstraete, David Ernsting, Stephen Dugdale, Peter Elliott, Marcin Dulak, José A. Flores Livas, Stefaan Cottenier, Yasushi Shinohara, Michael Fechner, and Yaroslav Kvashnin. The Elk FP-LAPW Code, http://elk.sourceforge.net/.

[18] Eberhard Engel and S. H. Vosko. Fourth-order gradient corrections to the exchange-only energy functional: Importance of $\nabla^2 n$ contributions. *Phys. Rev. B*, 50:10498–10505, 1994.

[19] Matthias Ernzerhof and Gustavo E. Scuseria. Assessment of the perdew–burke–ernzerhof exchange-correlation functional. *J. Chem. Phys.*, 110:5029–5036, 1999.

[20] Matthias Ernzerhof and Gustavo E. Scuseria. Kinetic energy density dependent approximations to the exchange energy. *J. Chem. Phys.*, 111:911–915, 1999.

[21] E. Fermi. *Rend. Acc. Naz. Lincei*, 6, 1927.

[22] Michael Filatov and Walter Thiel. Exchange-correlation density functional beyond the gradient approximation. *Phys. Rev. A*, 57:189, 1998.

[23] Michael Filatov and Walter Thiel. Tests of a density functional with Laplacian terms: activation barriers and bond-stretching energies. *Chem. Phys. Lett.*, 295:467–474, 1998.

[24] Antoine Georges, Gabriel Kotliar, Werner Krauth, and Marcelo J. Rozenberg. Dynamical mean-field theory of strongly correlated fermion systems and the limit of infinite dimensions. *Rev. Mod. Phys.*, 68:13–125, Jan 1996.

[25] P Giannozzi, O Andreussi, T Brumme, O Bunau, M Buongiorno Nardelli, M Calandra, R Car, C Cavazzoni, D Ceresoli, M Cococcioni, N Colonna, I Carnimeo, A Dal Corso, S de Gironcoli, P Delugas, R A DiStasio Jr, A Ferretti, A Floris, G Fratesi, G Fugallo, R Gebauer, U Gerstmann, F Giustino, T Gorni, J Jia, M Kawamura, H-Y Ko, A Kokalj, E Küçükbenli, M Lazzeri, M Marsili, N Marzari, F Mauri, N L Nguyen, H-V Nguyen, A Otero de-la Roza, L Paulatto, S Poncé, D Rocca, R Sabatini, B Santra, M Schlipf, A P Seitsonen, A Smogunov,

I Timrov, T Thonhauser, P Umari, N Vast, X Wu, and S Baroni. Advanced capabilities for materials modelling with quantum espresso. *Journal of Physics: Condensed Matter*, 29(46):465901, 2017.

[26] Paolo Giannozzi, Stefano Baroni, Nicola Bonini, Matteo Calandra, Roberto Car, Carlo Cavazzoni, Davide Ceresoli, Guido L Chiarotti, Matteo Cococcioni, Ismaila Dabo, Andrea Dal Corso, Stefano de Gironcoli, Stefano Fabris, Guido Fratesi, Ralph Gebauer, Uwe Gerstmann, Christos Gougoussis, Anton Kokalj, Michele Lazzeri, Layla Martin-Samos, Nicola Marzari, Francesco Mauri, Riccardo Mazzarello, Stefano Paolini, Alfredo Pasquarello, Lorenzo Paulatto, Carlo Sbraccia, Sandro Scandolo, Gabriele Sclauzero, Ari P Seitsonen, Alexander Smogunov, Paolo Umari, and Renata M Wentzcovitch. Quantum espresso: a modular and open-source software project for quantum simulations of materials. *Journal of Physics: Condensed Matter*, 21(39):395502 (19pp), 2009.

[27] P. Hohenberg and W. Kohn. Inhomogeneous electron gas. *Phys. Rev.*, 136(3B):B864–B871, Nov 1964.

[28] R. O. Jones and O. Gunnarsson. The density functional formalism, its applications and prospects. *Rev. Mod. Phys.*, 61:689–746, Jul 1989.

[29] J.-P. Julien and J. Bouchet. Ab-initio gutzwiller method: First application to plutonium. In Jean-Pierre Julien, Jean Maruani, Mayou Didier, Stephen Wilson, and Gerardo Delgado-Barrio, editors, *Recent Advances in the Theory of Chemical and Physical Systems*, pages 509–534, Dordrecht, 2006. Springer Netherlands.

[30] Peter J. Knowles and H.-J. Werner. An efficient second order MCSCF method for long configuration expansions. *Chem. Phys. Letters*, 115:259–267, 1985.

[31] Peter J. Knowles and H.-J. Werner. Internally contracted multiconfiguration reference configuration interaction calculations for excited states. *Theor. Chem. Acc.*, 84:95–103, 1992.

[32] W. Koch and M.C. Holthausen. *A chemist's guide to density functional theory*. Wiley-VCH, 2000.

[33] W. Kohn. Density functional and density matrix method scaling linearly with the number of atoms. *Phys. Rev. Lett.*, 76:3168–3171, Apr 1996.

[34] W. Kohn and L. J. Sham. Self-consistent equations including exchange and correlation effects. *Phys. Rev.*, 140(4A):A1133–A1138, Nov 1965.

[35] Stefan Kurth and John P. Perdew. Role of the exchange-correlation energy: Nature's glue. *International Journal of Quantum Chemistry*, 77(5):814–818, 2000.

[36] Stefan Kurth, John P. Perdew, and Peter Blaha. Molecular and solid-state tests of density functional approximations: LSD, GGAs, and meta-GGAs. *Int. J. Quantum Chem.*, 75:889–, 1999.

[37] N. D. Lang and W. Kohn. Theory of metal surfaces: Charge density and surface energy. *Phys. Rev. B*, 1:4555–4568, Jun 1970.

[38] N. D. Lang and W. Kohn. Theory of metal surfaces: Induced surface charge and image potential. *Phys. Rev. B*, 7:3541–3550, Apr 1973.

[39] David C. Langreth and M. J. Mehl. Beyond the local-density approximation in calculations of ground-state electronic properties. *Phys. Rev. B*, 28:1809–1834, Aug 1983.

[40] David C. Langreth and John P. Perdew. Theory of nonuniform electronic systems. i. analysis of the gradient approximation and a generalization that works. *Phys. Rev. B*, 21:5469–5493, Jun 1980.

[41] Chengteh Lee, Weitao Yang, and Robert G. Parr. Development of the colle-salvetti correlation-energy formula into a functional of the electron density. *Phys. Rev. B*, 37(2):785–789, Jan 1988.

[42] Mel Levy. Universal variational functionals of electron densities, first-order density matrices, and natural spin-orbitals and solution of the *v*-representability problem. *Proc. Nat. Acad. Sci.*, 76(12):6062–6065, 1979.

[43] Mel Levy. Electron densities in search of hamiltonians. *Phys. Rev. A*, 26:1200–1208, Sep 1982.

[44] Elliott H. Lieb. *Physics as Natural Philosophy*, page 111. MIT Press, Cambridge, 1982.

[45] Elliott H. Lieb. Density functionals for coulomb systems. *Int. J. Quantum Chem.*, 24(3):243–277, 1983.

[46] Jonathan E. Moussa. Minimax rational approximation of the fermi-dirac distribution. *The Journal of Chemical Physics*, 145(16):164108, 2016.

[47] J. P. Perdew and Alex Zunger. Self-interaction correction to density-functional approximations for many-electron systems. *Phys. Rev. B*, 23(10):5048–5079, 1981.

[48] John P. Perdew. Density-functional approximation for the correlation energy of the inhomogeneous electron gas. *Phys. Rev. B*, 33:8822–8824, Jun 1986.

[49] John P. Perdew, Kieron Burke, and Matthias Ernzerhof. Generalized gradient approximation made simple. *Phys. Rev. Lett.*, 77(18):3865–3868, Oct 1996.

[50] John P. Perdew, Stefan Kurth, Aleš Zupan, and Peter Blaha. *Phys. Rev. Lett.*, 82:2544–, 1999.

[51] John P. Perdew, Adrienn Ruzsinszky, Gábor I. Csonka, Lucian A. Constantin, and Jianwei Sun. Workhorse semilocal density functional for condensed matter physics and quantum chemistry. *Phys. Rev. Lett.*, 103:026403–, 2009. Erratum: Phys. Rev. Lett. **106**, 179902 (2011).

[52] John P. Perdew and Yue Wang. Accurate and simple density functional for the electronic exchange energy: Generalized gradient approximation. *Phys. Rev. B*, 33:8800–8802, Jun 1986.

[53] John P. Perdew and Yue Wang. Accurate and simple analytic representation of the electron-gas correlation energy. *Phys. Rev. B*, 45(23):13244–13249, Jun 1992.

[54] J. M. Pitarke and A. G. Eguiluz. Jellium surface energy beyond the local-density approximation: Self-consistent-field calculations. *Phys. Rev. B*, 63:045116, Jan 2001.

[55] E. I. Proynov, A. Vela, and D. R. Salahub. Nonlocal correlation functional involving the Laplacian of the density. *Chem. Phys. Lett.*, 230:419–428, 1994.

[56] I. V. Solovyev, P. H. Dederichs, and V. I. Anisimov. Corrected atomic limit in the local-density approximation and the electronic structure of d impurities in rb. *Phys. Rev. B*, 50:16861–16871, Dec 1994.

[57] P. J. Stephens, F. J. Devlin, C. F. Chabalowski, and M. J. Frisch. *J. Phys. Chem.*, 98:11623, 1994.

[58] Jianwei Sun, John P Perdew, and Adrienn Ruzsinszky. Semilocal density functional obeying a strongly tightened bound for exchange. *Proc. Nat. Acad. Sci.*, 112:685–9, 2015.

[59] Jianwei Sun, Adrienn Ruzsinszky, and John P. Perdew. Strongly Constrained and Appropriately Normed Semilocal Density Functional. *Phys. Rev. Lett.*, 115:036402–, 2015.

[60] Jianmin Tao, John P. Perdew, Viktor N. Staroverov, and Gustavo E. Scuseria. Climbing the density functional ladder: Nonempirical meta–generalized gradient approximation designed for molecules and solids. *Phys. Rev. Lett.*, 91:146401, Sep 2003.

[61] L.H. Thomas. The calculation of atomic fields. *Math. Proc. Camb. Phil. Soc.*, 23(05):542–548, 1927.

[62] Troy Van Voorhis and Gustavo E. Scuseria. A novel form for the exchange-correlation energy functional. *J. Chem. Phys.*, 109:400–410, 1998.

[63] S. H. Vosko, L. Wilk, and M. Nusair. Accurate spin-dependent electron liquid correlation energies for local spin density calculations: a critical analysis. *Can. J. Phys.*, 58(8):1200–1211, 1980.

[64] Zidan Yan, John P. Perdew, and Stefan Kurth. Density functional for short-range correlation: Accuracy of the random-phase approximation for isoelectronic energy changes. *Phys. Rev. B*, 61:16430–16439, Jun 2000.

[65] Yan Zhao and Donald G. Truhlar. A new local density functional for main-group thermochemistry, transition metal bonding, thermochemical kinetics, and noncovalent interactions. *J. Chem. Phys.*, 125:194101, 2006.

Appendix A

Derivation of the Exchange Functional for Confinement Physics

Parametrization of the Exchange Functional

The parametrization of the LDA is given by

$$[l\,\varepsilon_{\mathrm{X}}(n(\mathbf{r}),|\nabla n(\mathbf{r})|,\mathrm{ELF}(\mathbf{r}))]^{\mathrm{LDA}} = -\frac{3}{4\pi}\left(3\sqrt{\pi}\exp[-\bar{z}^2]\alpha(n(\mathbf{r}),|\nabla n(\mathbf{r})|,\mathrm{ELF}(\mathbf{r}))\right)^{1/3}\,. \tag{A.1}$$

The parametrization of the HOG reference system is somewhat more involved, it is given by

$$[l\,\varepsilon_{\mathrm{X}}(n(\mathbf{r}),|\nabla n(\mathbf{r})|,\mathrm{ELF}(\mathbf{r}))]^{\mathrm{conf}} = \frac{a_0(\alpha)+a_2(\alpha)\bar{z}^2+a_4(\alpha)\bar{z}^4+a_6(\alpha)\bar{z}^6-\bar{z}^8}{-\bar{z}^8/[2\sqrt{2\alpha}\,l\,\varepsilon_{\mathrm{X}}^{>}(2\sqrt{2\alpha}\,\bar{z})]+1}\,. \tag{A.2}$$

where we use the exchange energy in the limit of large $\bar{z}$ denoted by

$$\varepsilon_{\mathrm{X}}^{>}(t) = \frac{1}{t}\left[\frac{1}{2}-\frac{I_1(t)}{t}+\frac{L_1(t)}{t}\right]\,. \tag{A.3}$$

The various auxiliary functions are defined as

$$a_0(\alpha) = 2A(\alpha)\,, \tag{A.4}$$

$$a_2(\alpha) = \frac{B(\alpha)}{2(\alpha)}-2A(\alpha)\,, \tag{A.5}$$

$$a_4(\alpha) = \frac{C(\alpha)}{48\alpha^2}-\frac{B(\alpha)}{2\alpha}+A(\alpha)\,, \tag{A.6}$$

$$a_6(\alpha) = \frac{D(\alpha)}{2880\alpha^3}-\frac{C(\alpha)}{48\alpha^2}+\frac{B(\alpha)}{4\alpha}-\frac{A(\alpha)}{3}\,, \tag{A.7}$$

$$\tag{A.8}$$

and

$$A(\alpha) = \frac{1-\gamma-\ln(-2\alpha)-\Gamma(0,-2\alpha)}{4\sqrt{\pi}} - \frac{2\sqrt{2\alpha}}{3\pi} + \frac{1-e^{2\alpha}}{8\sqrt{\pi}\alpha} - \frac{4(2\alpha)^{3/2}}{45\pi}\,{}_2F_2\left(1,\frac{3}{2};\frac{5}{2},\frac{7}{2};2\alpha\right) \tag{A.9}$$

$$B(\alpha) = \frac{e^{2\alpha}\,\mathrm{erfc}(\sqrt{2\alpha})-2\alpha-1}{\sqrt{\pi}} + \frac{2\sqrt{2\alpha}}{\pi} \tag{A.10}$$

$$C(\alpha) = \frac{16\alpha^2}{\sqrt{\pi}}\left[e^{2\alpha}\,\mathrm{erfc}(\sqrt{2\alpha})-1\right] \tag{A.11}$$

$$D(\alpha) = \frac{128\alpha^3}{\sqrt{\pi}}\left[2(1+\alpha)\,e^{2\alpha}\,\mathrm{erfc}(\sqrt{2\alpha}) - \sqrt{2\alpha/\pi}-2\right], \tag{A.12}$$

where γ is Euler's constant, $\Gamma(s,t)$ is an upper incomplete gamma function, $\mathrm{erfc}(t)$ is the complementary error function, $I_n(t)$ is the modified Bessel function of first kind, $L_n(t)$ is the modified Struve function, and ${}_pF_q\left(a_1,\ldots,a_p;b_1,\ldots,b_q;t\right)$ is the generalized hypergeometric function. The parametrization in Equation (A.2) depends on the density, its gradient, and the ELF through the parametrization of the confinement factor

$$\alpha\left(n(\mathbf{r}),|\nabla n(\mathbf{r})|,\mathrm{ELF}(\mathbf{r})\right) = \left\{ e^{-\alpha_1 s^2(\mathbf{r})}\left[\frac{\beta_1 \frac{D(\mathbf{r})}{D^{\mathrm{LDA}}(\mathbf{r})}}{1+e^{\alpha_2\left(\beta_1\frac{D(\mathbf{r})}{D^{\mathrm{LDA}}(\mathbf{r})}-\beta_2\right)}} + \frac{\beta_2^2\left(\beta_1\frac{D(\mathbf{r})}{D^{\mathrm{LDA}}(\mathbf{r})}\right)^{-1}}{1+e^{\alpha_2\left(-\beta_1\frac{D(\mathbf{r})}{D^{\mathrm{LDA}}(\mathbf{r})}+\beta_2\right)}}\right]\right. \tag{A.13}$$

$$\left. + \left(1-e^{-\alpha_1 s^2(\mathbf{r})}\right)\beta_1\frac{D(\mathbf{r})}{D^{\mathrm{LDA}}(\mathbf{r})}\right\}\frac{\bar{z}^2(|\nabla n(\mathbf{r})|,ELF(\mathbf{r}))}{s^2(\mathbf{r})} \tag{A.14}$$

where we express the dimensionless coordinate $\bar{z}$ in terms of a Lambert function $W(t)$ as

$$\bar{z}^2(|\nabla n(\mathbf{r})|,ELF(\mathbf{r})) = \frac{1}{2}W\left[18\pi\left(\beta_1\frac{D(\mathbf{r})}{D^{\mathrm{LDA}}(\mathbf{r})}\right)^2 s^2(\mathbf{r})\right], \tag{A.15}$$

and the values of the various parameters $\alpha_1 = 100/7$, $\alpha_2 = 200$, $\beta_1 = 3/5$, and $\beta_2 = (9\pi)^{-1/3}$.

The Electron Localization Function

The ELF [9] is measure for characterizing the localization of electron within molecules and solids. It is defined as

$$ELF(\mathbf{r}) = \frac{1}{1+\left[D(\mathbf{r})/D^{\mathrm{LDA}}(\mathbf{r})\right]^2}, \tag{A.16}$$

where the ratio is given by

$$\frac{D(\mathbf{r})}{D^{\mathrm{LDA}}(\mathbf{r})} = \bar{\tau}(\mathbf{r}) - \frac{5}{3}s(\mathbf{r})^2 \tag{A.17}$$

with the dimensionless density gradient

$$s(\mathbf{r}) = \frac{|\nabla n(\mathbf{r})|}{2(3\pi^2)^{1/3} n^{4/3}(\mathbf{r})} \tag{A.18}$$

and the dimensionless ratio

$$\bar{\tau}(\mathbf{r}) = \frac{\tau(\mathbf{r})}{\tau^{\mathrm{LDA}}(\mathbf{r})} \tag{A.19}$$

of the kinetic energy density $\tau(\mathbf{r})$ and the LDA of the kinetic energy density $\tau^{\mathrm{LDA}}(\mathbf{r}) = (3/10)(3\pi^2)^{2/3} n^{5/3}(\mathbf{r})$. An illustration of the ELF for a material containing d electrons is shown in Figure A.

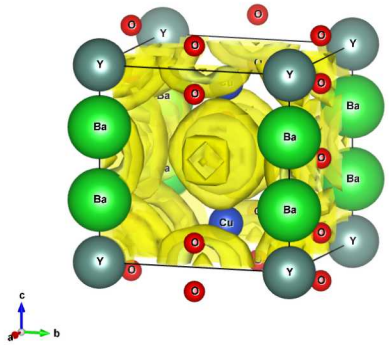

Figure A.1. Illustration of the ELF in Yttrium barium copper oxide as a representative example of a material containing localized d electrons.

DISTRIBUTION:

1 Ann E. Mattsson, XCP-5, Mailstop F644
Los Alamos National Laboratory
Los Alamos, NM

1 MS 0889 Wahid L. Hermina, 01850
1 MS 0613 David Ingersoll, 02500
1 MS 0887 Terrence L. Aselage, 01800
1 MS 0359 Donna L. Chavez, LDRD Office, 01171
1 MS 0899 Technical Library, 9536 (electronic copy)


Sandia National Laboratories